PMMA-Fe_3O_4 for internal mechanical support and magnetic thermal ablation of bone tumors

Kexiao Yu[1,2#], Bing Liang[2#], Yuanyi Zheng[3]*, Agata Exner[4], Michael Kolios[5], Tiantian Xu[6], Dajing Guo[7], Xiaojun Cai[3], Zhigang Wang[2], Haitao Ran[2], Lei Chu[1]* and Zhongliang Deng[1]*

1 Department of Orthopaedics, Second Affiliated Hospital of Chongqing Medical University, 76 Linjiang Road, Yuzhong Distinct, Chongqing, 400010, P. R. China.

2 Chongqing Key Laboratory of Ultrasound Molecular Imaging, Second Affiliated Hospital of Chongqing Medical University, 76 Linjiang Road, Yuzhong Distinct, Chongqing, 400010, P. R. China.

3 Shanghai Institute of Ultrasound in Medicine, Shanghai Jiao Tong University Affiliated Sixth People's Hospital, 600 Yishan Road, Xuhui Distinct, Shanghai, 200233, P. R. China.

4 Radiology department of University Hospital, Case Western Reserve University, 10900 Euclid Ave, Cleveland, OH, 44106, USA.

5 Department of Physics, Ryerson University, Toronto, 350 Victoria Street Toronto, Ontario M5B 2K3, Ontario, Canada

6 Guangdong Provincial Key Laboratory of Robotics and Intelligent System, Shenzhen Institutes of Advanced Technology, Chinese Academy of Sciences, Shenzhen 518055, China

7 Department of Radiology, Second Affiliated Hospital of Chongqing Medical University, 76 Linjiang Road, Yuzhong Distinct, Chongqing, 400010, P. R. China.

# These authors contributed equally to this work.

* Corresponding authors: Prof.Yuanyi Zheng, Shanghai Institute of Ultrasound in Medicine, Shanghai Jiao Tong University Affiliated Sixth People's Hospital, 600 Yishan Road, Xuhui Distinct, Shanghai, 200233, P. R. China. E-mail: zhengyuanyi@163.com; Dr. Lei Chu, Second Affiliated Hospital of Chongqing Medical University, 76 Linjiang Road, Yuzhong Distinct, Chongqing, 400010, P. R. China. E-mail: Chulei2380@163.com; Prof. Zhongliang Deng, Second Affiliated Hospital of Chongqing Medical University, 76 Linjiang Road, Yuzhong Distinct, Chongqing, 400010, P. R. China. E-mail: zhongliang.deng@yahoo.com.

Supplementary Information

Materials and Methods

Preparation of magnetic PMMA bone cement

The PMMA powder (26 g) was composed of PMMA (14.2 g), zirconium dioxide (11.7 g) and benzoyl peroxide (0.1 g). The liquid monomer (10 mL) consisted of methyl methacrylate (9.2 g) and N, N-dimethyl-p-toluidine (0.2 g). The PMMA powder and MMA monomer were obtained from a clinical manufacturer (OSTEOPAL® V, Heraeus, Ltd, Germany). The ratio of PMMA (weight) to MMA monomer (volume) was 2.6 w/v per the manufacturer's instructions. Magnetic PMMA bone cement was prepared by adding the Fe_3O_4 magnetic NPs (CAS:1317-61-9, Chengdu AikeDa Chemical Reagent Co., Ltd., China) to the PMMA powder at an iron/total weight of 3%, 6% and 9%. The PMMA powder and Fe_3O_4 NPs were placed into an EP tube (volume: 5 mL) and distributed uniformly with a vortex mixer (Vortex.Genie2T, Scientific Industries, Ltd, U.S.A.) at 3000 rpm continuously for 30 s, then mixed with MMA monomer (the density of the MMA monomer was 0.94 g/mL as indicated in the instruction manual). The response time for mixing the powder with the monomer was 1.5 min.

Morphology characterization of PMMA-Fe_3O_4 bone cement

The morphologies of the PMMA powder, MMA monomer, Fe_3O_4 NPs and the prepared magnetic polymethylmethacrylate bone cement (PMMA-Fe_3O_4) in a syringe were recorded in digital photos. The microstructures of Fe_3O_4 NPs, PMMA powder and PMMA-6%Fe_3O_4 were characterized by scanning electron microscopy (SEM,

JSM-7900F, JEOF Ltd., Japan) at an accelerating voltage of 1 kV. The microstructure of polymerized PMMA-Fe_3O_4 was characterized by scanning electron microscopy (SEM, vega3, Tescan Ltd., Czech) at an accelerating voltage of 15 kV. Elemental analysis was performed by energy dispersive X-ray spectrometry (SEM, JSM-7900F, JEOF Ltd., Japan) at an accelerating voltage of 10 kV.

Evaluation of injectability of PMMA-Fe_3O_4 bone cement

The injectability of PMMA, PMMA-3%Fe_3O_4, PMMA-6%Fe_3O_4 and PMMA-9%Fe_3O_4 bone cement paste was evaluated by the "injectable percentage" [1]. In short, the mixed bone cement was placed in a 1-mL syringe (the inner diameter of the needle was 1.2 mm). The extrusion force was measured with a 3-kN force transducer at a speed of 15 mm/min **(Figure S2E)**. When the extrusion force reached 70 N or all of the bone cement (1 mL) was squeezed out, the extrusion force test was terminated [2]. The injectable percentage was calculated by the following formula:

Injectable percentage= $(V_{inj} / V_{total}) \times 100\%$

V_{inj}: The volume of injected PMMA of the syringe (volume: 1 mL).

V_{total}: The total volume of PMMA in the syringe before injection.

Exothermic temperature and setting time of PMMA-Fe_3O_4 bone cement

The maximum setting temperature and setting time were measured with a common protocol [3]. The PMMA-3%Fe_3O_4, PMMA-6%Fe_3O_4, PMMA-9%Fe_3O_4 and PMMA mixtures and the monomer were manually mixed for 1.5 min at room temperature (26 ± 0.5 °C), and 0.2 mL sample was then placed in a 1-mL syringe. A thermocouple (type K, class 1, diameter 0.25 mm) was inserted into the center of the material to

record the temperature every 10 s as the material polymerized. As specified by ISO5833:2002(E), the maximum temperature (Tmax) was recorded directly, and the setting time (Tset) was the time taken to reach the temperature midway between room temperature and Tmax.

Mechanical properties of PMMA-Fe_3O_4 bone cement

Compressive strength test

In accordance with the ISO5833:2002(E), the anti-compression capability was evaluated. The PMMA, PMMA-3%Fe_3O_4, PMMA-6%Fe_3O_4 and PMMA-9%Fe_3O_4 bone cement pastes were poured into cylindrical column molds made from polytetrafluoroethylene (PTFE) and stainless steel caps **(Figure S3)**. Setting yielded plasticity specimens (6 mm in diameter and 12 mm in length), which were dried for 24 h at room temperature. The samples were compressed by a static and dynamic fatigue testing machine (Instron 3365; Intron Corp., St. Paul, MN, U. S. A.) with a 3-kN load-cell, at a crosshead displacement speed of 20 mm/min to obtain the load-displacement curves. The compressive strength was calculated with the following formula:

$P_c = F / A$

P_c: Compressive strength.

F: Ultimate compressive force.

A: Compressive area of the cylinder materials. $A = \pi r^2$

where F was acquired from the load-displacement curve, and r was measured by a digital Vernier caliper.

Three-point bending test

As ISO5833:2002(E) guideline, PMMA, PMMA-3%Fe_3O_4, PMMA-6%Fe_3O_4 and PMMA-9%Fe_3O_4 bone cement paste were poured into square moulds made from PTFE and stainless steel caps **(Figure S3)**. Setting yielded plasticity specimens (3.3 mm in thickness, 10 mm in width and 75 mm in length), which were dried for 24 h at room temperature. The samples were placed in a static and dynamic fatigue testing machine (Instron 3365; Intron Corp., St. Paul, MN, U.S.A.), loaded and subjected to a constant displacement of 5 mm/min until failure occurred; and the support span was 60 mm. The bending strength and bending modulus (slope between 5 and 35 N) were calculated from the recorded load-deflection curve using the following formulas:

$\sigma_f = 3PL / 2bd^2$

$E_f = L^3m / 4bd^3$

σ_f: Bending strength in outer fibers at midpoint (MPa)

E_f: Bending modulus (MPa)

P: Load at a given point on the load-deflection curve (N)

L: Support span (mm)

b: Width of test beam (mm)

d: Depth of tested beam (mm)

m: The slope of the initial straight-line portion of the load-deflection curve (N/mm)

***In vitro* magnetic-thermal-induced thermal efficiency evaluation**

Four types of PMMA containing different volumes and different amounts of Fe_3O_4 (0.15 mL of 0%, 0.15 mL of 3%, 0.15 mL of 6%, 0.15 mL of 9%, 0.10 mL of 6% and 0.2 mL of 6%) were manually shaped into small balls, dried for 24 h at room

temperature, and then placed into Eppendorf tubes (2 mL) containing 1.5 mL of saline solution. All four types of PMMA were exposed to an AMF by a homemade magnetic hyperthermia analyzer (frequency: 626 KHz, output current: 28.6 A, turns of coil: 2, coil length: 1 cm, field amplitude: 5.72 K/Am) for 180 s [4]. The peak surface temperatures of saline solutions were recorded with every 10 s by a far-infrared thermometer (FOTRIC225, ZXF Laboratories, U.S.A.) during exposure to the AMF. The thermal images were analyzed via AnalyzIR 7.1 software (ZXF Laboratories, U.S.A.). The specific absorption ratio (SAR) value for Fe in PMMA-6%Fe_3O_4 was calculated under this AMF.

Evaluation of magnetic-thermal-induced temperature distribution in *ex vivo*

PMMA-6%$Fe_3O_4$was selected for further study based on the above experiments. One hundred fifty microliters of PMMA-6%Fe_3O_4 (m_{Fe}: 0.01 g) was manually shaped into small balls, cut into two halves, and dried for 24 h at room temperature. The hemispheric PMMA-6%Fe_3O_4 was embedded into a 4 cm × 2 cm × 2 cm piece of excised bovine liver with the flat surfaces of the hemispheric sections parallel to the surface of the excised bovine liver, and the pieces were then exposed to an AMF for 180 s. The peak surface temperature of the liver block at different distances (0 mm, 0.5 mm, 1 mm, 1.5 mm, 2 mm, 2.5 mm, 3 mm, 3.5 mm, 4 mm, 4.5 mm and 5 mm away from the surface of the hemisphere) was recorded every 10 s by a far-infrared thermometer during 180 s of heating. The thermal images were analyzed via AnalyzIR 7.1 software (ZXF Laboratories, U. S. A.).

***Ex vivo* magnetic-thermal-induced ablation efficiency evaluation**

A total of 150 μL of PMMA-6%Fe_3O_4 (m_{Fe}: 0.01 g) was manually shaped into small balls and dried for 24 h at room temperature. The balls were embedded into the freshly bovine liver piece (2 cm × 2 cm × 2 cm) and then exposed to the same AMF for 120 s, 150 s and 180 s. As mentioned in the previous section, thermal images were acquired. The ablated bovine liver pieces were cut through the middle into two halves and the mean distance to ablated tissue (from the surface of PMMA-6%Fe_3O_4 to the border between normal and ablated liver tissue) was observed and recorded in digital photos. The mean distance to ablated tissue was calculated by the following formula:

$D_a = (D_l + D_s) / 2$

D_a: Ablation diameter.

D_l: Long distance of the ablated tissue.

D_s: Short distance of the ablated tissue.

Biosafety of PMMA-6%Fe_3O_4 bone cement

PMMA-6%Fe_3O_4 bone cement was manually shaped into small ball samples. After solid phase transition, the samples were disinfected by an ultraviolet lamp for 30 min, and then 0.3 mL of PMMA-6%Fe_3O_4 bone cement sample was placed into 10 mL of medium for 24 h to obtain the PMMA-6%Fe_3O_4 solution medium. Human umbilical vein endothelial cells (UVECs) were cultured in a 6-well plate with high-glucose Dulbecco's modified Eagle’s medium (DMEM) supplemented with 1% penicillin/streptomycin and 10% fetal bovine serum (FBS) in an incubator with an atmosphere containing 5% CO_2 at 37 °C. After incubation for 24 h, 3 mL of PMMA-6%Fe_3O_4 solution medium was added into the experimental wells, and 3 mL of normal

medium was added into the control wells. After incubation for an additional 24 h, the cells were collected and preserved by the addition of 1 mL of PBS into the tubes. The samples were then prepared for the cell apoptosis test through flow cytometry evaluation [5].

A total of 150 μL of PMMA-6%Fe_3O_4 (m_{Fe}: 0.01 g) was injected into the lateral thigh muscles of 9 New Zealand white rabbits (2 months old, weight of 2.0-2.5 kg, any sex). Six rabbits were randomly selected for blood collection. Three-milliliter blood specimens were collected through the ear-veins of rabbits at preinjection, day 1, day 7, day 14, day 21 and day 28. From the 3-mL blood specimens, 1 mL was preserved for a blood test, and the other 2 mL was centrifuged at 3000 r/min speed for 8 min to collect the supernatant for the serum test. After 28 days, the other three rabbits were sacrificed to collect the major organs, including the heart, liver, spleen, lung, kidney and muscle tissue around the PMMA-6%Fe_3O_4, for pathological examination. The organs and tissue slices were stained with hematoxylin-eosin (H&E) after fixation in a 4% paraformaldehyde solution for 48 h; the H&E slices were then observed by optical microscopy (Olympus BX53, TB Tokyo, Japan). The blood tests included white blood cell (WBC), red blood cell (RBC), hemoglobin (HB) and platelet (PLT) counts, which were measured by an animal fully automatic blood cell analyzer (BC-2800vet Shenzhen MINDRAY Bio Medical Electronic Limited by Share Ltd, China) and compared to normal reference values. The serum tests included measurements of alanine aminotransferase (ALT), aspartate aminotransferase (AST), creatinine (CR), blood urea nitrogen (BUN), creatine kinase (CK) and lactate dehydrogenase levels

(LDH-L), which were performed by ELISA kits (CO52, CO72, CO74, CO10, CO59 and CO18, respectively; Changchun Huili Biotech Co., Ltd., China).

In order to investigate any escape of the Fe_3O_4 NPs, inductively coupled plasma optical emission spectrometer (ICP-OES) quantitative measurements were performed as follows. The first same batch of 0.3 mL of PMMA-6%Fe_3O_4 was divided into two equal parts: 0.15 mL of PMMA-6%Fe_3O_4 was immediately measured by ICP-OES after it solidified and dried for 24 h. Another 0.15 mL of PMMA-6%Fe_3O_4 was injected into the tibial plateau of a tumor-planted rabbit under CT guidance and heated for 150 s. After 1 month, the implanted and heated PMMA-6%Fe_3O_4 was taken out and measured by ICP-OES. Prussian blue staining of the organs in the control group (healthy rabbits) and PMMA-6%Fe_3O_4 group after heating for 30 days was also performed. The second same batch of 0.3 mL of PMMA-6%Fe_3O_4 was also divided into two equal parts: 0.15 mL of PMMA-6%Fe_3O_4 was immediately measured by ICP-OES after it solidified and dried for 24 h. Another 0.15 mL of PMMA-6%Fe_3O_4 was injected into a beaker full of PBS, and a strong $Nd_2Fe_{14}B$ magnet was applied to attract the PMMA-6%Fe_3O_4 behind the beaker glass for 1 month. Then, the sample was measured by ICP-OES. The ICP-OES results for the iron concentrations in the paired parts were compared to detect the escape of Fe_3O_4 NPs.

Preparation of a tumor model in the rabbit tibial plateau with a VX2 tumor mass

New Zealand white rabbits, which were 2 months old and weighed 2.0-2.5 kg, were used for the experiment. All animal procedures were performed in accordance with the Guidelines of the Ministry of Science and Technology of Health Guide for Care and

Use of Laboratory Animals, China, and approved by the institutional ethical committee (IEC) of Second Affiliated Hospital of Chongqing Medical University. Food and drink were withheld for 6 h before anesthesia for all experimental rabbits. The weight was recorded, and the skin on the knee was prepared. The cryopreserved primary tumor mass (1 mL/3 g) came from the Animal Laboratory Center of Chongqing Medical University. After fast thawing in warm water (37 °C), the tumor mass was cut into small masses (approximately 0.5 mm^3) on a clean bench. These small masses were resuspended with 1 mL of PBS and then transferred to a 2-mL syringe (with 1-mm diameter needle). Finally, these VX2 tumor masses were injected into the lateral thigh of a two-month-old rabbit, generating the tumor-bearing rabbit. After 4 weeks, the volume of the tumor was large enough to establish the VX2 tumor model.

After the tumor-bearing rabbit was euthanized using appropriate approved methods and skin degerming, a 5-cm longitudinal skin incision was made on the lateral thigh. The whole tumor mass was harvested under careful dissection. The tumor mass was cut in half, and the fresh white fish-like tumor tissue was identified and located between the inner necrotic tissue and the outer healthy muscle tissue. The fresh white fish-like tumor tissue was dissected and cut into small blocks (approximately 1 mm^3). The experimental rabbits received general anesthesia using 3% pentobarbital solution, and then a marrow puncture needle (inner diameter of 1 mm and outer diameter of 1.2 mm) was used for a vertical puncture in the medial cortical bone of the tibial plateau; the needle insertion depth was limited to 7 mm by the depth restrictor of

the marrow puncture needle. Then, the inner core of the needle was pulled out, and 1 tumor block was coaxially pushed into the tibial plateau via the blunt side of a K-wire (diameter 1 mm, **Figure S8**). Finally, a 4-mm piece of gelatin sponge (Xiang en Medical Technology Development Co., Ltd., Jiangxi, China) was inserted to seal the needle tract. The needle was removed and pressed at the puncture point for 5 min. CT examinations were performed on day 13, day 14 or day 15, when the volume of destroyed bone reached 180.0±15.0 mm^3, measured in the CT images. The rabbits were then prepared for subsequent procedures.

***Ex vivo* compressive test of the tibial plateau**

Twelve tumor-bearing and four healthy rabbits were chosen for this experiment. The twelve tumor-bearing rabbits were randomly divided into 3 groups. For the PMMA-6%Fe_3O_4-Heating (PMMA-6%Fe_3O_4-H) and PMMA-6%Fe_3O_4 groups, four rabbits were randomly selected and anesthetized, and then 150 μL of PMMA-6%Fe_3O_4 (m_{Fe}: 0.01 g) bone cement paste was injected into the tumor under CT guidance (Aquilion ONE, 320-row, Toshiba Corp., Japan, 200 mA and 120 KV, slice thickness and slice interval were each 0.5 mm). The tumor-bearing legs in the PMMA-6%Fe_3O_4-H group were exposed to an AMF as above for 150 s, while the other tumors in the PMMA-6% Fe_3O_4 group were not exposed. For the Tumor group, no materials were injected into the tumors. For the Normal group, 4 legs without tumors were harvested from the four healthy rabbits.

At 24 h following injection, 16 rabbits were euthanized with an overdose of pentobarbital. The lower legs were harvested, and soft tissue was removed. The bones

were then fixed on a static and dynamic fatigue testing machine (Instron 3365; Intron Corp., St. Paul, MN, U.S.A.) for a compression test with a load and a constant displacement of 20 mm/min until failure occurred **(Figure S3)**. The ultimate compressive strength and compressive stiffness were calculated from the recorded load-displacement curve. The stiffness was determined from the slope of the initial straight-line portion of the load-displacement curve.

***In vivo* magnetic-thermal-induced ablation efficiency**

The tumor-bearing New Zealand white rabbits were divided into four groups (n=20 in each group) and were anesthetized via the rabbit ear vein with 3% pentobarbital solution. Before intervention, all tumor-planted rabbits were examined by contrast-enhanced nuclear magnetic resonance (Achieva 3.0 T TX, Philips Corp., Netherlands) and CT (Aquilion ONE, 320-row, Toshiba Corp., Japan). For the PMMA-6%Fe_3O_4-H group, rabbits were randomly selected, and 150 μL of PMMA-6%Fe_3O_4 (m_{Fe}: 0.01 g) was injected into the tumors under CT guidance. After injection, the tumor was heated simply by placing the tumor-bearing part of the leg into a water-cooled magnetic induction coil for 150 s. For the Tumor-H group, these rabbits were exposed to AMF without injection of PMMA-6%Fe_3O_4 bone cement. The surface skin temperature of the tibial plateaus was continuously measured by the same far-infrared thermometer as described above. For the PMMA-6%Fe_3O_4 group, 150 μL of PMMA-6%Fe_3O_4 (m_{Fe}: 0.01 g) was injected into the tumors as described above, and for the untreated Tumor group, 150 μL of saline was injected into the tumors instead of PMMA-6%Fe_3O_4. On the first day after injection, three rabbits in each group were randomly selected and

euthanized for tumor pathological examination by H&E straining. On day 4 after injection, 3 rabbits in each group were randomly selected and euthanized, and terminal deoxynucleotidyl transferase dUTP nick end labeling (TUNEL) and a proliferating cell nuclear antigen (PCNA) assay for tumor cell apoptosis and proliferation, respectively, were performed through immunohistochemistry. The apoptotic index (AI) and proliferation index (PI) were calculated. The ration of the number of positively stained cells to the total number of tumor cells was calculated in five randomly selected, equal-sized fields. Three rabbits in each group were randomly selected, and 2 mL of blood was collected through the ear vein of rabbits at preinjection and on day 1, day 4, day 7 and day 14. The samples were centrifuged at 3000 r/min speed for 8 min, and the supernatants were collected and preserved at -80 °C until serum samples were used to evaluate the expression of heat shock protein 70 (HSP-70) and interleukin 2 (IL-2).

All the remaining 14 rabbits in each group were fed for further observation of the tumor growth trend through CT examination and measurement of the knee perimeter on day 1, day 4, day 7, day 14, day 21, day 28, day 35, day 42, day 49 and day 56 after treatment. The destroyed bone volume of the tibial plateau in all rabbits was calculated from CT images and compared with the preinjection image, and the knee perimeter was measured using a soft ruler. For the PMMA-6%Fe_3O_4 group, the thickness of the upper tibial plateau cortical bone was measured by CT imaging, and the CT value of the upper tibial plateau cortical bone was also measured by CT imaging. During the follow-up, any rabbits that had died were dissected to check metastasis to viscera. At the end of the experiment, all rabbits were euthanized using appropriate approved

methods. The mortality and the percentage of visceral metastasis were calculated.

Statistical analysis

All quantitative results are given as the mean ± standard deviation. An independent t-test and one-way ANOVA were used for intergroup comparisons. A paired t-test was used to compare the data between the preintervention and each follow-up time point with the SPSS program package. Probability levels of < 0.05 and < 0.001 were considered to be the thresholds for significance (***: mean statistically significant difference of $p < 0.001$; *: mean statistically significant difference of $p < 0.05$).

Reference:

1. Burguera EF , Xu HHK , Sun L. Injectable calcium phosphate cement effects of powder-to liquid ratio and needle size. J Biomed Mater Res B Appl Biomater. 2008; 84: 493-502.

2. Christof B, Stefan B, Christian S, Volkmar J, Bernd W. A biomechanical evaluation of the epidural neurolysis procedure. Pain Physician. 2012; 15: 89-97.

3. Schroder C, Nguyen M, Kraxenberger M, Chevalier Y, Melcher C, Wegener B, et al. Modification of PMMA vertebroplasty cement for reduced stiffness by addition of normal saline: a material properties evaluation. Eur Spine J. 2017; 26: 3209-15.

4. Chen Y, Jiang L, Wang R, Lu M, Zhang Q, Zhou Y, et al. Injectable smart phase-transformation implants for highly efficient in vivo magnetic-hyperthermia regression of tumors. Adv Mater. 2014; 26: 7468-73.

5. Wang F, Yang Y, Ling Y, Liu J, Cai X, Zhou X, et al. Injectable and thermally

contractible hydroxypropyl methyl cellulose/Fe3O4 for magnetic hyperthermia ablation of tumors. Biomaterials. 2017; 128: 84-93.

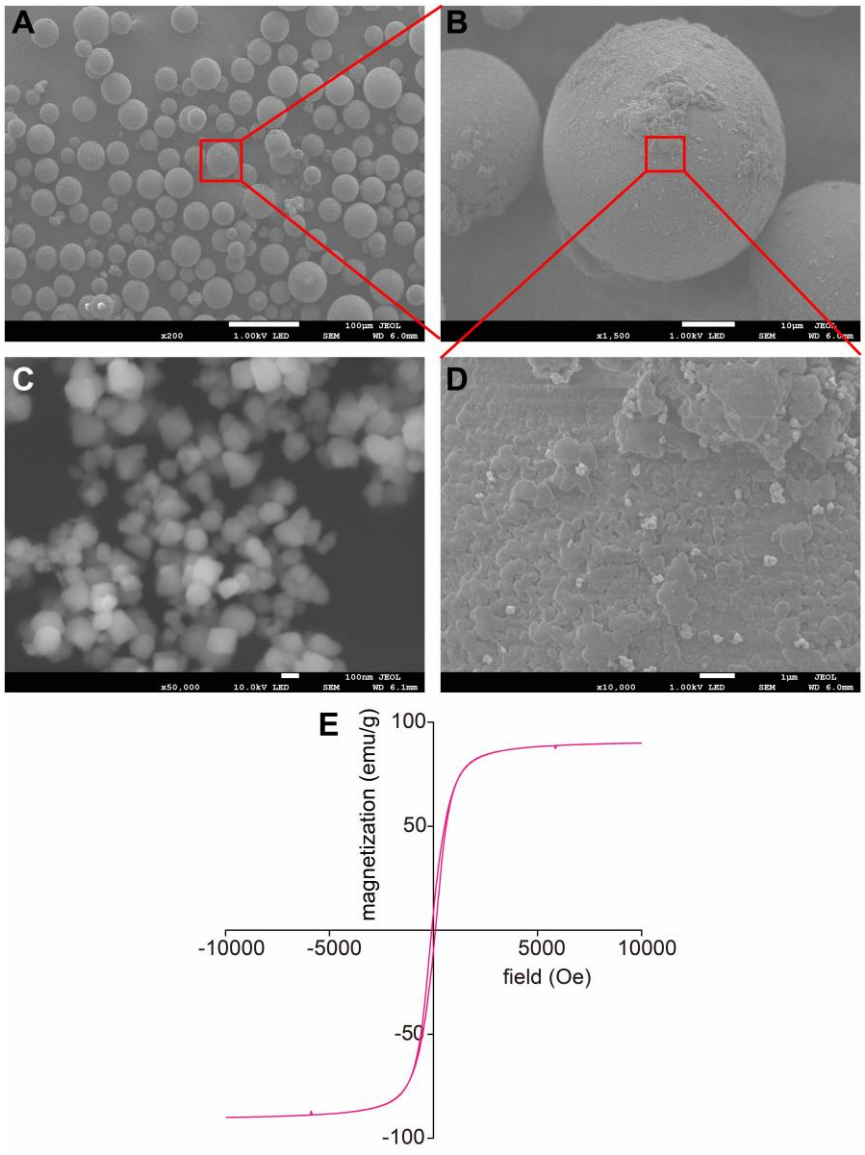

Figure S1. (A, B, D) Magnification SEM images of mixed PMMA powders and 6%Fe_3O_4 NPs. The scale bars are 100 µm, 10 µm and 1 µm, respectively. (C) Magnification SEM images of Fe_3O_4 NPs. The scale bar is 100 nm. (E) Magnetic hystersis loop of pure Fe_3O_4 nanoparticles.

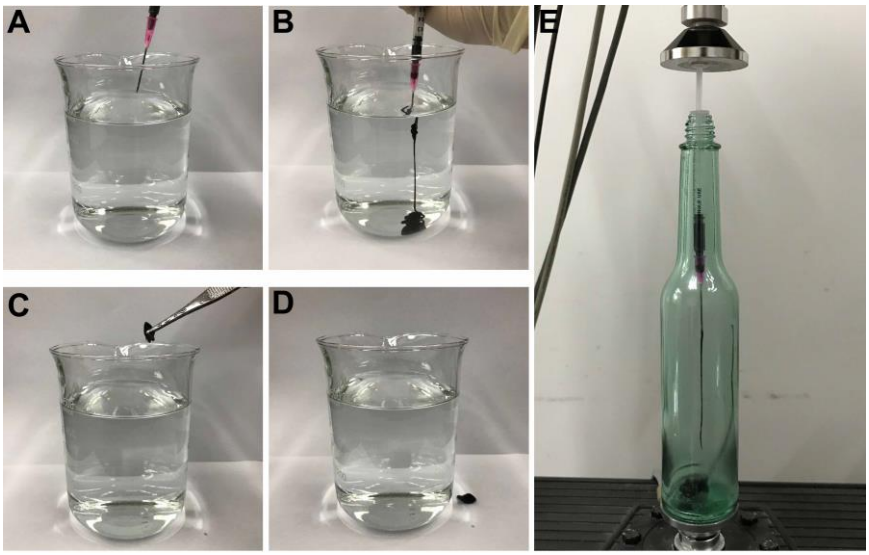

Figure S2. Photographic images of injectable PMMA-6%Fe_3O_4 bone cement (A) before, (B) in progress, (C) after contacting water and (D) after transforming to solid phase. (E) Photograph of the progress for evaluating injectability.

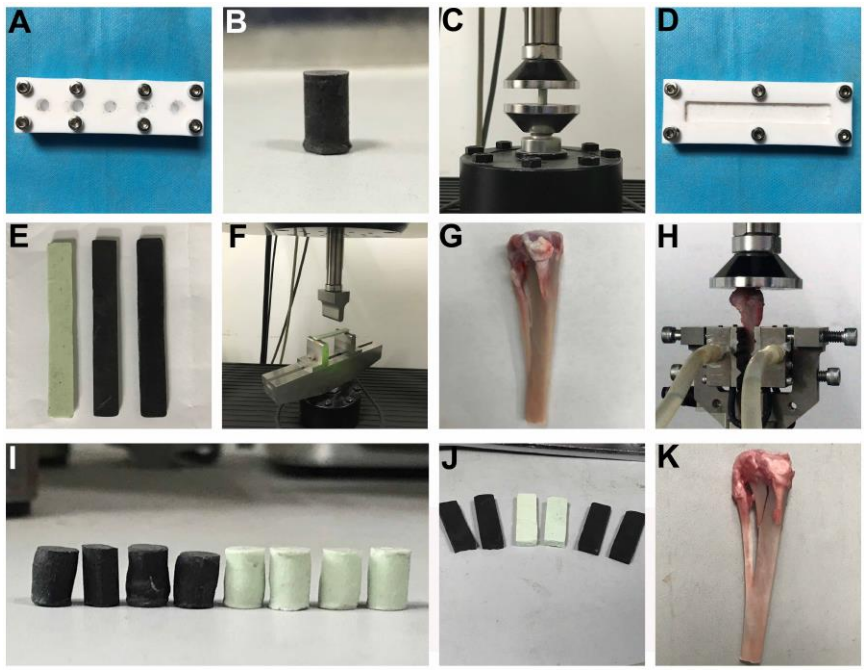

Figure S3. (A) Digital image of the cylindrical columns molds. (B) The cylindrical column plasticity specimens (6 mm in diameter and 12 mm in length). (C) Compressive strength test of column plasticity specimens. (D) Digital picture of the

square column molds. (E) Representative square plasticity specimens (3.3 mm in thickness, 10 mm in width and 75 mm in length). (F) Progress of three-point bending test of square plasticity specimens. (G) The harvested tibial segment. (H) Compressive test of the tibial plateau. (I) The fractured cylindrical column plasticity specimens. (J) The fractured representative square plasticity specimens. (K) The fractured rabbit tibial plateau.

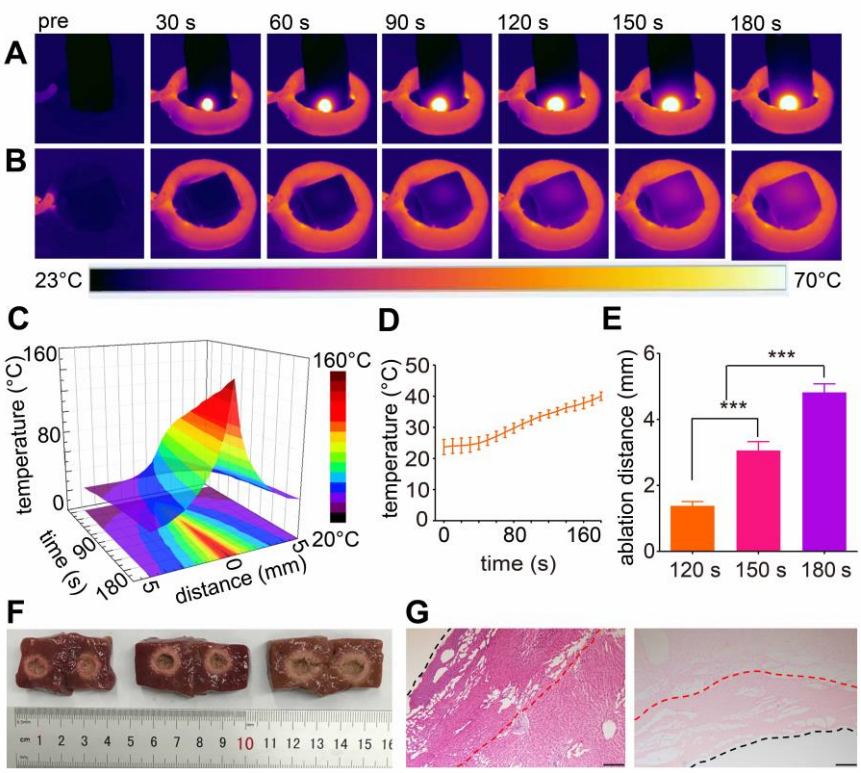

Figure S4. (A) Thermal images of the 2 cm x 2 cm x 4 cm excised bovine liver embedded hemisphere of 75 μL of PMMA-6%Fe_3O_4 and (C) the corresponding temperature-time-distance plot. (B) Thermal images of the 2 cm x 2 cm x 2 cm excised bovine liver containing 150 μL of PMMA-6%Fe_3O_4 and (D) the corresponding temperature-time curve. (E) Visual ablation distance of excised bovine containing 150 μL of PMMA-6%Fe_3O_4 after 120 s, 150 s and 180 s of magnetic thermal ablation. (F) Macroscopic digital photos of excised bovine liver in AMF for 120 s, 150 s and 180 s,

respectively. (G) H&E staining and Prussian blue staining in excised bovine liver after ablation. (red dotted line means the edge of ablation, and black dotted line means the edge of removed PMMA-6%Fe_3O_4. The scale bar is 200 μm).

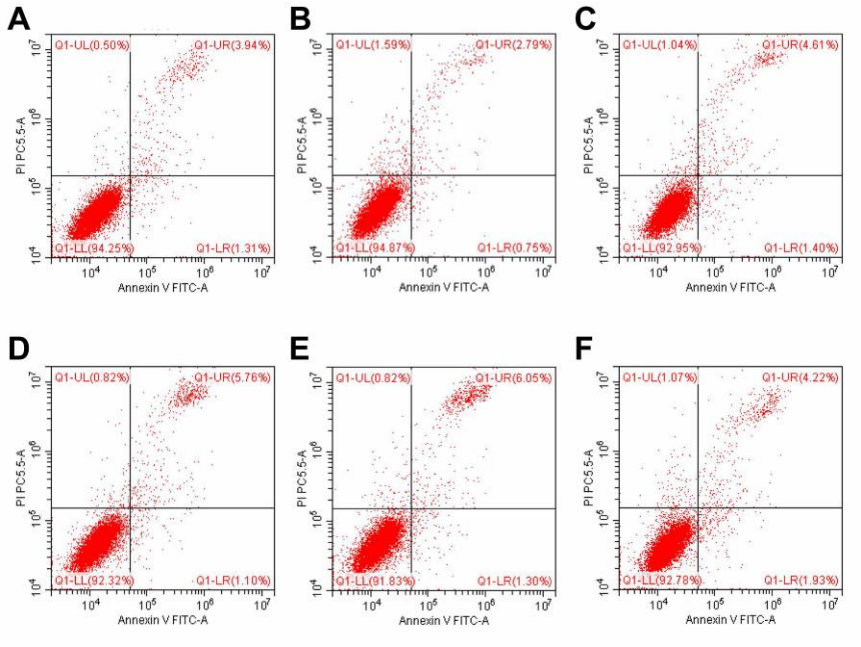

Figure S5. The cell apoptosis results measured by flow cytometry in the control group (A-C) and experimental group (D-F).

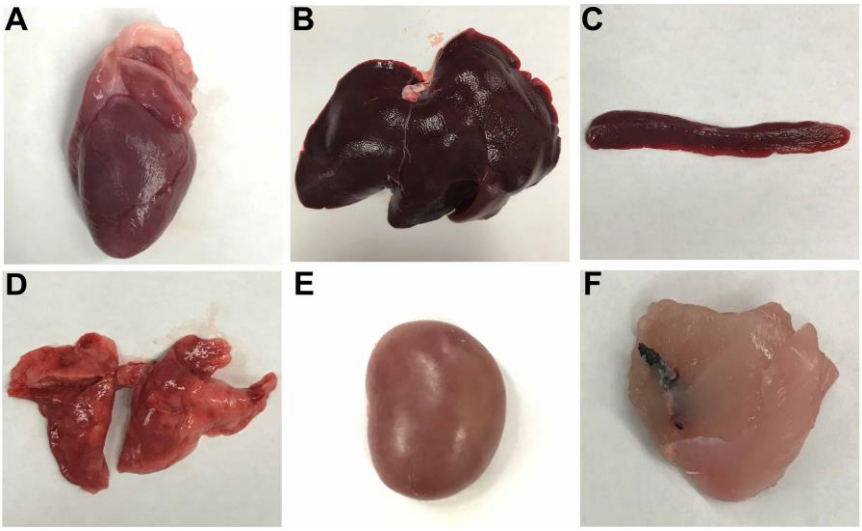

Figure S6. Digital photos of rabbit viscera including (A) heart, (B) liver, (C) spleen,

(D) lung, (E) kidney and (F) muscle tissue around the PMMA-6%Fe_3O_4 in the biocompatibility and biosafety test.

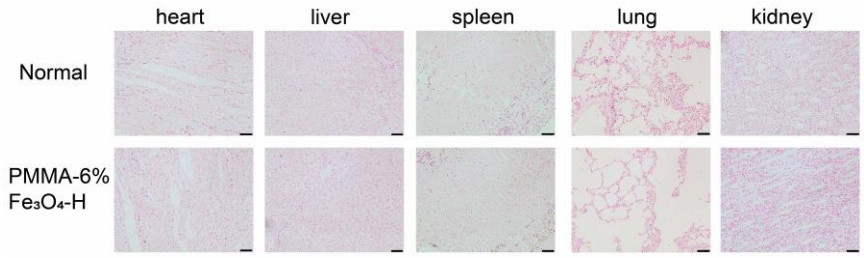

Figure S7. Prussian blue staining of the organs in the control group (healthy rabbits) and PMMA-6%Fe_3O_4 group after heating for 30 days. The scale bar is 100 μm.

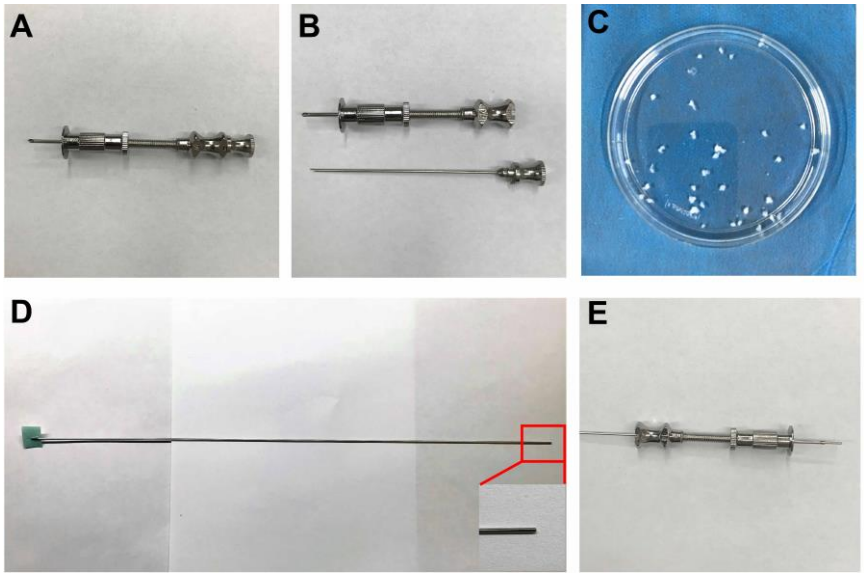

Figure S8. (A) A marrow puncture needle with the core in was used to puncture the tibial plateau; the depth restrictor was set to 7 mm. (B) Marrow puncture needle with the removal of the core. (C) Fresh tumor tissue mass blocks (approximately 1 mm^3). (D) The blunt side of the K-wire was used to push the tumor blocks into the tibial plateau through the marrow puncture needle. Inset: the operating part. (E) Complex K-wire and the marrow needle.

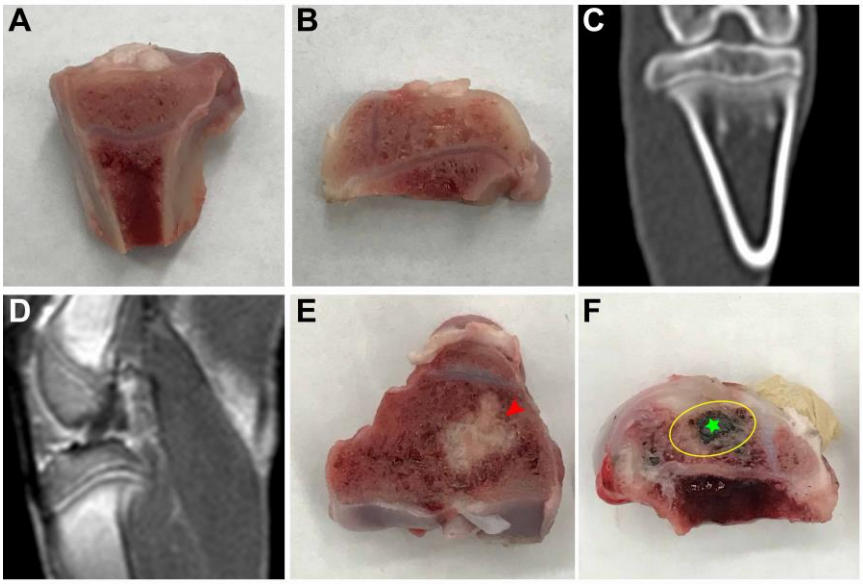

Figure S9. (A) Digital photo of coronal incised normal tibial plateau. (B) Digital photo of sagittal incised normal tibial plateau. (C) Coronal CT image of normal tibial plateau. (D) Sagittal enhanced MRI image of normal tibial plateau. (E) Digital photo of transversal incised tumor-bearing tibial plateau. (red arrow: the white VX2 tumor tissues in the cancellous bone of tibial plateau.) (F) Digital photo of sagittal incised post-heating tibial plateau. (green star: the solid PMMA-6%Fe_3O_4, yellow circle: the ablated tumor tissue.)

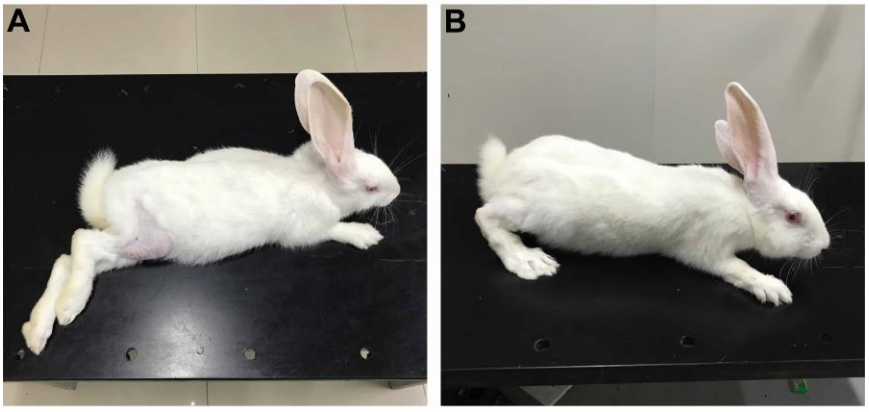

Figure S10. (A) Photograph of rabbit in the PMMA-6%Fe_3O_4 group on day 21, posed in a strained posture. (B) Photograph of rabbit in the PMMA-6%Fe_3O_4-H group on

day 21, posed in a normal posture.

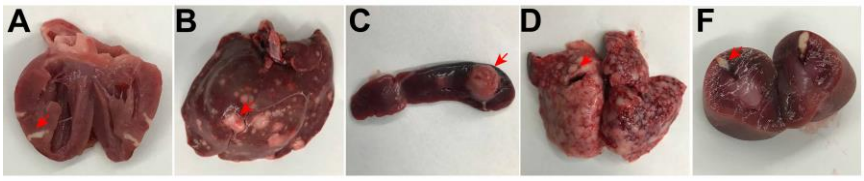

Figure S11. Digital photos of metastasized viscera include (A) heart, (B) liver, (C) spleen, (D) lung, (E) kidney. (red arrow: metastatic tumor tissues.)

Table S1. Blood test analysis before and after injection PMMA-6%Fe_3O_4 bone cement for day 1, day 7, day 14, day 21 and day 28.

	WBC（10^9/L）	RBC（10^{12}/L）	HGB（g/L）	PLT（10^9/L）
Reference ranges	5.20~13.5×10^9	5.00~7.60×10^{12}	105.00~170.00	100.00~712.00
Pre	6.97 ± 2.46	6.07 ± 0.48	124.33 ± 7.09	527.67 ± 356.73
Day 1	6.20 ± 0.36	6.07 ± 0.52	119.67 ± 10.97	392.33 ± 311.74
Day 7	7.67 ± 0.84	4.70 ± 0.32	82.67 ± 12.01	292.33 ± 217.73
Day 14	10.20 ± 3.58	6.63 ± 1.59	97.00 ± 6.08	646.67 ± 194.53
Day 21	9.27 ± 1.55	5.10 ± 0.45	100.67 ± 9.45	470.00 ± 219.34
Day 28	6.53 ± 0.60	6.13 ± 0.53	131.33 ± 15.18	448.67 ± 263.23

Values are the mean ± SD (n = 6).